The Growth of HF Polymers in Helium Nanodroplets: Probing the Barriers to Ring Insertion

G. E. Douberly and R. E. Miller*

Department of Chemistry, University of North Carolina, Chapel Hill, North Carolina 27599

Received: November 1, 2002; In Final Form: March 3, 2003

We report the first experimental observation of $(HF)_n$ ($n = 4,5,6$) clusters, grown in helium nanodroplets. The structures of these complexes are determined from infrared laser spectroscopy, recorded in the spectral region from 3100 to 3900 cm^{-1}. Comparisons with previous gas-phase spectra and ab initio calculations indicate that the helium-solvated tetramer is cyclic, suggesting that the barrier to inserting an HF into a preformed cyclic trimer is small. In contrast, the cyclic pentamer is not observed. Instead, we observe four of the five H−F stretching vibrational bands of a new isomer of $(HF)_5$, corresponding to a tetramer ring to which a fifth HF is hydrogen bonded. A large static electric field is used to establish that this $(HF)_5$ isomer is indeed polar and to measure the angle between the permanent dipole moment and the transition dipole moments for these vibrations. These vibrational transition dipole moment angles (VTMAs) and the corresponding vibrational frequencies are also calculated at the MP2/6-311++G(3df,3pd) level of theory. Comparisons between the experimental and calculated VTMAs and the vibrational frequencies provide convincing evidence for the formation of this "4 + 1" isomer. The results are rationalized in terms of the available intermolecular potentials for these systems.

Introduction

Recent studies in helium nanodroplets have revealed that the growth of clusters under these low-temperature conditions can lead to the formation of metastable species.[1−3] We have explained this in terms of the fact that the helium acts to efficiently quench the condensing molecules so that the system's internal energy remains low at all times. Thus if the system enters a local minimum on the potential energy surface, it may become trapped there, the helium having cooled the system before it can surmount the barrier to the global minimum. Examples of this include the formation of long chains of HCN[2] and HCCCN[1] and the cyclic isomer of $(H_2O)_6$.[3,4] Experiments of this type can provide us with insights into the barriers between minima on a complex energy landscape and aid in understanding the pathways for rearranging hydrogen-bonding networks, such as those controlling the dynamics of liquid water. In the present study we investigate the formation of $(HF)_n$ clusters in helium for $n > 2$.

Hydrogen fluoride clusters have been the subjects of extensive experimental and theoretical studies and have become benchmark systems for the study of hydrogen bonding. The dimer is of particular interest, given that it provides a means of directly probing the pair potential. In addition, it undergoes wide amplitude tunneling, making the corresponding spectroscopic observations particularly sensitive to the barrier between the equivalent minima on the potential surface. The structure and tunneling dynamics of the HF dimer were originally studied experimentally using microwave spectroscopy.[5,6] Other vibrational states of the dimer have subsequently been studied using near[7−10] and far[11] infrared spectroscopy. Photodissociation experiments have also been carried out for several different excited vibrational states,[12,13] providing detailed information on both the dissociation energy of the dimer and its state-to-state dynamics. This extensive database has inspired many theoretical studies, with the result being the development of accurate potential surfaces[14] that quantitatively reproduce essentially all of the data. Most recently, we have carried out a rotationally resolved infrared study of the HF dimer solvated in helium nanodroplets,[15] the goal being to study the effects of the solvent on the vibrational/tunneling dynamics of the dimer.

It is now well established, from both experiment[16−24] and theory,[25−31] that the most stable isomers of the larger polymers of HF are all cyclic, at least up to $n = 7$. A recent combined experimental/theoretical study of the H−F out-of-plane libration fundamental band of the tetramer provided conclusive evidence for its cyclic structure.[32] Although the H−F stretch vibrational spectrum of $(HF)_3$ is not rotationally resolved, the $(DF)_3$ spectrum does show rotational fine structure which confirms its cyclic structure.[17,18] Indeed, the cyclic structures of these complexes are all well established.

A previous study of the HF trimer in helium droplets confirmed that the cyclic structure is formed by sequential HF pick-up.[15] By studying larger clusters ($n \geq 4$), we address here the issue of whether molecules that approach a preformed cyclic complex in helium can insert into the ring. This is clearly necessary if the cyclic motif is to be continued, as seen for $(H_2O)_n$ previously.[4] If not, we would expect to observe a new class of structures, consisting of a cyclic ring with one or more HF molecules attached on the outside. In the present study the structures of the complexes formed in helium are determined by infrared laser spectroscopy. We make use of a large electric field to aid in the assignment of the observed spectra. This method is based on the use of a polarized laser, aligned either parallel or perpendicular to the applied field. If the complex possesses a permanent dipole moment, it will be oriented with the applied field. Under these conditions, the angle between the vibrational transition moment for various modes and the

* Corresponding author.

10.1021/jp022360+ CCC: $25.00
Published on Web 04/22/2003

TABLE 1: Harmonic Vibrational Frequencies, ω, Intensities, and the VTMAs, α_{calc}, Calculated at the MP2/6-311++G(3df,3pd) Level of Theory, for Various HF Complexes[a]

isomer	ω cm^{-1}	int. km/mol	ω_{scal} cm^{-1}	ν_{exp} cm^{-1}	α_{calc} degrees	α_{exp} degrees
trimer	3891.5	1345.3	3709.0	3709		
3 + 1	3673.9	608.8	3501.6		40.8	
	3864.2	500.2	3683.0		77.2	
	3988.3	471.9	3801.3		8.8	
	4056.4	297.9	3866.2		2.0	
tetramer	3617.6	3613.7	3447.9	3438		
4 + 1	3329.5	730.3	3173.9	3174	33.0	
	3553.2	1314.5	3386.6	3385	83.8	72 ± 5
	3659.1	1234.0	3487.5	3489	15.5	22 ± 5
	3780.0	640.3	3602.7	3593	39.7	49 ± 3
	4077.1	349.2	3885.9	3876.1	2.1	35 ± 2

[a] The harmonic frequencies were scaled by a factor of 0.953103, determined from the ratio of the experimental, ν_{exp}, and calculated trimer vibrational frequencies. The experimentally determined VTMAs, α_{exp}, were obtained by the polarization ratio procedure described in the text.

permanent dipole moment can be determined from the ratio of the signal intensities obtained with the two laser polarization directions. The experimentally determined vibrational transition moment angles (VTMAs) and vibrational band origins are compared to ab initio values, also reported here. As shown below, these results provide unambiguous structural information for the system studied here.

We find that the addition of a fourth molecule to a droplet containing a cyclic HF trimer results in ring insertion and the formation of a cyclic tetramer. Nevertheless, the addition of a fifth molecule results in the formation of the "4 + 1" complex, namely a tetramer ring with the fifth molecule hydrogen-bonded to one of the fluorine atoms in the ring. These experimental results are in good agreement with recent theoretical calculations of the transition state energies between these "n + 1" and cyclic structures.[26]

Computational Method

There have been numerous calculations of the structures and relative energies of various isomers of the $(HF)_n$ complexes.[25−31] Unfortunately, vibrational frequencies have only been reported for some of these, and the VTMAs needed in the present study have not been reported. As a result, we carried out ab initio MP2 calculations for a number of the important species using a 6-311++G(3df,3pd) basis set.[33] Table 1 summarizes the vibrational frequencies, intensities, and VTMAs for the cyclic trimer and tetramer, along with the "3 + 1" and "4 + 1" complexes. A scale factor of 0.953103 was used to bring the calculated harmonic vibrational frequency of the cyclic trimer into agreement with the known vibrational band center in helium droplets, namely 3709 cm^{-1}. The harmonic frequencies calculated for the other complexes were then scaled using the same scale factor.

Experimental Method

A detailed description of the apparatus used in the present study can be found elsewhere,[34] so that only a brief description is given here. Helium droplets were formed by expanding ultrahigh purity (99.9999%) helium gas through a 5-μm diameter nozzle operated at 20 K. The stagnation pressure behind the nozzle was maintained at approximately 50 atm, resulting in the formation of droplets with a mean diameter of approximately 7 nm (4000 atoms).[35,36] After passing through a skimmer, the droplets enter a 4-cm-long pick-up cell. A needle value was used to regulate the flow of HF into the cell, and the pressure was varied to control the number of molecules captured by the droplets.[37] The seeded droplets then pass through a multipass/Stark cell, where laser excitation occurs. Downstream of the laser interaction region is a bolometer detector, used to measure the energy of the helium beam.

A cw F-center laser was used to vibrationally excite the H−F stretches of the complexes formed in the droplets, and subsequent vibrational relaxation resulted in the evaporation of several hundred helium atoms (5 cm^{-1} per atom).[38] The absorption spectrum was then obtained by recording the reduction in the flux of helium atoms to the bolometer.[34] The spectrum was made background free by modulating the laser and using phase-sensitive detection methods. To cover the entire range of the HF cluster spectrum, it was necessary to use both crystal No. 2 (KCl:Li) and No. 3 (RbCl:Li), pumped by 3 W and 1.4 W of all-lines red from a krypton ion laser. Details on the tuning and calibration of the laser frequency can be found elsewhere.[8]

A set of Stark electrodes was positioned orthogonal to the multipass cell, and a large DC electric field was applied to the laser interaction region.[1] The laser electric field direction was aligned either parallel or perpendicular to the applied field direction. This was useful in the case of the "n + 1" complexes, which possess a large permanent electric dipole moment. Although the vibrational bands observed here are not rotationally resolved, and the band shapes are unaffected by the field, the intensity of the bands change upon application of the field.[39,40] For the case of a small VTMA, with the laser polarization parallel to the applied field, the intensity of the band increases upon application of the field. For large VTMAs (>54.75°) the intensity decreases in parallel polarization. The electric field was calibrated by recording a Stark spectrum of the R(1) transition of gas-phase HCN using the same electrode configuration. This was done by turning off the helium droplet beam and increasing the HCN pressure in the pick-up cell so that it acted like an effusive source of gas-phase molecules. These measurements yielded a field of 41.26 kV/cm for the experiments reported here.

Experimental Results

Figure 1 shows a comparison between the spectrum of HF polymers formed in helium droplets with that of the gas-phase (molecular beam) spectrum. Similar gas-phase spectra have been reported previously,[20,21,23,24] and the assignment of the various bands to the cyclic clusters is well established. There are clearly significant differences between the two spectra, the first qualitative indication that cluster formation in helium is indeed different from that in a free jet expansion. Two of the peaks in the helium-droplet spectrum are easily assigned to the cyclic trimer and tetramer, as indicated in the figure. Note that the gas-phase spectrum shown in the figure was recorded using conditions where the larger clusters are optimized and the trimer is not observed. Nevertheless, the trimer spectrum is well-known [16,17,41,42] and the assignment is clear. Supporting this assignment is the fact that the helium-solvated trimer band is completely unaffected by the electric field, indicating that the corresponding complex is nonpolar, as is certainly the case for the HF trimer.[5,25,43] The gas-phase trimer band is centered at 3712 cm^{-1}, while in the helium droplet spectrum it is located at 3709 cm^{-1}, corresponding to a solvent shift of 3 cm^{-1}.

The largest peak in the helium spectrum is assigned to the cyclic tetramer. Anharmonic frequency calculations yield a fundamental HF stretching frequency for the cyclic tetramer of 3433 cm^{-1}, [20] in good agreement with the corresponding helium

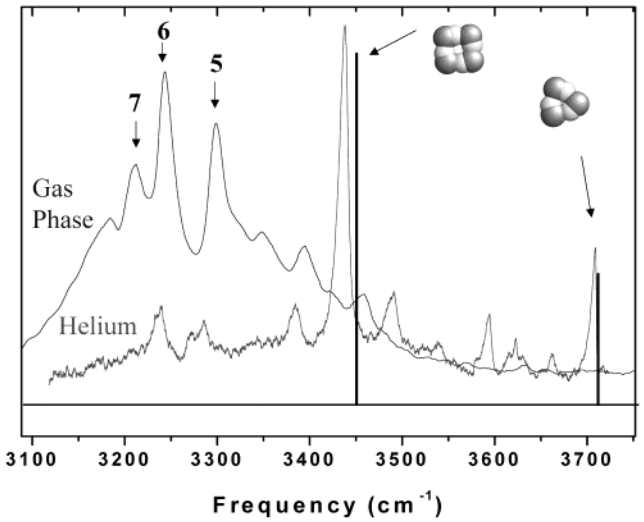

Figure 1. A comparison between the IR spectrum of HF polymers formed in helium droplets and that of the corresponding gas phase (molecular beam) species. The stick spectrum corresponds to the scaled vibrational frequencies and intensities for the cyclic trimer and tetramer determined from the ab initio calculations. A scale factor of 0.953103 is applied to the calculated harmonic frequencies, as needed to bring the calculated trimer frequency into agreement with the experimental result. The ab initio intensities were scaled to agree with the experimental intensity of the tetramer. The HF pick-up cell pressure was optimized for the pick-up of four HF molecules. The calculated and experimental tetramer/trimer intensity ratios are 2.69 and 2.71, respectively.

droplet frequency, namely 3437 cm^{-1}. Ab initio harmonic frequency calculations were carried out as part of the present work and were scaled to agree with the experimental trimer frequency. The same scale factor used for the tetramer gives excellent agreement with the experimental result, as shown by the vertical bars in Figure 1. The heights of these bars represent the calculated transition moments of the two complexes, the relative intensities also being in good agreement with experiment. Note that the conditions used to record the helium droplet spectrum were optimized for forming the tetramer. Under these conditions, the concentration of trimer, tetramer, and pentamer in the droplets will be rather similar. The same intensity scale factor was used for all of the complexes considered here. Once again, application of an electric field did not change the intensity of the tetramer band.

It is interesting that the tetramer band is not evident in the gas-phase spectrum. This observation has been discussed previously in the literature and is thought to be the result of the fact that the tetramer has a larger dissociation energy than the corresponding HF vibrational energy.[44−47] As a result, in the gas phase the tetramer likely does not dissociate in the vibrationally excited state. Although the bolometer used in these studies could in principle see the corresponding increase in energy associated with vibrational excitation of the complex, the sensitivity for this type of detection is lower than for the case where the complex dissociates.[21] In the case of the helium droplet spectrum, detection is no problem because dissociation of the complex is not necessary, but only vibrational relaxation leading to evaporation of helium.

Because the average time between pick-up events is rather long (∼50 ms, on the basis of a droplet beam velocity of 200 m/s and a pick-up cell length of 4 cm, optimized for the pick-up of four molecules), we can be rather confident that the trimer ring is already formed and cooled by the time the fourth molecule is captured. Thus the observation of the cyclic tetramer

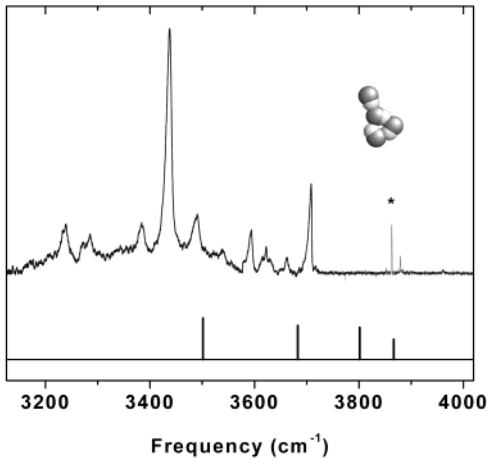

Figure 2. The spectrum of HF polymers in helium droplets compared to the stick spectrum of the scaled ab initio vibrational frequencies and intensities for the "3 + 1" isomer. The scale factors determined from the calculated trimer frequency and the calculated tetramer intensity are used throughout. The * identifies the HF dimer band near 3862 cm^{-1}.

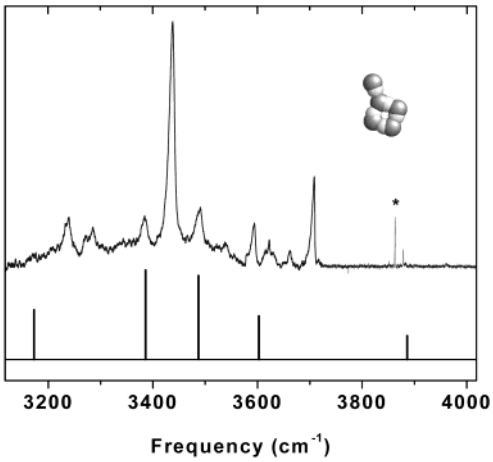

Figure 3. A comparison of the HF polymer spectrum with the stick spectrum of the scaled ab initio vibrational frequencies and intensities of the "4 + 1" isomer. The * identifies the HF dimer complex. The power output of the F-center laser begins to drop off below 3200 cm^{-1}, so that the band near 3174 cm^{-1} is barely visible.

indicates that ring insertion is indeed occurring in this case. To test this further, we carried out ab initio calculations for the "3 + 1" complex, scaling the frequencies as discussed above. The resulting spectrum is compared with the experimental results in Figure 2. The band that is predicted at 3801.3 cm^{-1} is completely absent in the experimental spectrum, indicating that the ring insertion process completely dominates and that the "3 + 1" isomer is not stabilized by the helium.

In the gas-phase spectrum, the bands that are centered at 3302 and 3245 cm^{-1} correspond to the nonpolar cyclic pentamer and hexamer, respectively.[20,21] This is consistent with the fact that they are completely unaffected by the application of a large electric field. Although two bands are observed in the helium droplet spectrum in this general region (namely at 3235 cm^{-1} and 3280 cm^{-1}), they are assigned to polar complexes, given that they do respond to the field. We can therefore conclude that the cyclic clusters larger than the tetramer are not formed in helium droplets (to within our sensitivity limits). The implication is clearly that the pick-up of a fifth HF does not result in ring insertion into the existing cyclic tetramer.

Figure 3 shows a comparison between the scaled ab initio vibrational spectrum for the "4 + 1" complex and the

experimental results. The resulting frequencies are compared in Table 1. In this case, the agreement is reasonable, certainly within the errors in the scaled harmonic vibrational frequencies. Once again, the intensities of the five bands for the "4 + 1" are scaled the same as for the cyclic tetramer. It is important to note that the lowest frequency band is near the end of the tuning range of the laser and the power in this region was quite low, perhaps accounting for the weakness of this band. Although the comparisons between the experimental and calculated frequencies and intensities give a rather convincing assignment for the "4 + 1" complex, this assignment is unambiguously confirmed in the next section using the VTMAs.

Determination of Vibrational Transition Dipole Moment Angles

In a recent paper[48] we reported the first results using a new method for determining VTMAs (α), applied to the study of the structure of isolated biomolecules. The basic experimental measurement is of the ratio of the integrated areas for a give vibrational band with the laser polarization aligned parallel and perpendicular to the applied electric field, namely $\rho(\alpha) = A_{||}(\alpha)/A_{\perp}(\alpha)$. The application of this approach to the determination of electronic transition moment directions has been described in detail previously.[49−51] The polarization ratio can be expressed in terms of the VTMA (α) as

$$\rho(\alpha) = \frac{\int_0^{\pi} P(\cos\theta)[2 - \sin^2\alpha - 2\cos^2\theta + 3\cos^2\theta\sin^2\alpha]\sin\theta\, d\theta}{2\int_0^{\pi} P(\cos\theta)[2\cos^2\theta + \sin^2\alpha - 3\cos^2\theta\sin^2\alpha]\sin\theta\, d\theta} \quad (1)$$

where θ is the angle between the permanent dipole moment direction and the *Z*-axis, defined as the direction of the applied field, in the laboratory frame. In high fields the dipole moment vector of the molecule precesses about the electric field. The orientation distribution for the permanent dipole,

$$P(\cos\theta) = \frac{1}{2}(1 + \sum_{n=1}^{\infty} a_n P_n(\cos\theta)) \quad (2)$$

is determined from a variational treatment of an asymmetric top in an electric field. This theoretical treatment, a detailed account of which is given elsewhere,[52,53] is for the most general case where the permanent dipole is not parallel to a principal axis. Briefly, symmetry-adapted symmetric top wave functions in the inertial frame are used as basis functions in this variational calculation,

$$|JKMs\rangle = \frac{1}{\sqrt{2}}(|JKM\rangle + (-1)^s|J - KM\rangle) \quad (3)$$

where $K > 0$, $s = 0$ or 1. The Hamiltonian for an asymmetric top in a uniform electric field is

$$H = BJ^2 + (A - B)J_z^2 + \frac{(C - B)}{4}(J_+^2 + J_-^2 + J_+J_- + J_-J_+) + \mu_p\cdot\mathbf{E} \quad (4)$$

A unitary transformation of the Hamiltonian matrix in the inertial frame gives a Hamiltonian matrix in the dipole frame,

$$\hat{H}' = D(\theta_m,\varphi_m)^+ \hat{H} D(\theta_m,\varphi_m) \quad (5)$$

The dipole frame is defined such that the permanent dipole is the *z*-axis in the molecular frame, and therefore θ_m and φ_m are Euler angles of μ_p in the inertial frame. Diagonalization of the Hamiltonian matrix in the dipole frame yields the energies, $E_{\tau M}$, and expansion coefficients, $C_{J,K,s}^{\tau,M}$, of the wave functions of the asymmetric top in a uniform electric field,

$$|\tau M\rangle = \sum_{J,K,s} C_{J,K,s}^{\tau,M}|JKMs\rangle_d \quad (6)$$

where τ is simply a register and $|JKMs\rangle_d$ are basis functions in the dipole frame. Knowledge of the energies and expansion coefficients completes the evaluation of the dipole distribution function, eq 2, where $P_n(\cos\theta)$ are Legendre polynomials, and a_n is given by the expression

$$a_n = \frac{(2n+1)}{2}\sum_M N_M \sum_\tau e^{-E\tau_M/k_BT} \sum_{J_1,J_2,K,s_1,s_2} C_{J_1Ks_1}^{\tau M} \times C_{J_2Ks_2}^{\tau M}[1 + (-1)^{s_1+s_2+J_1+J_2+n}] \times (-1)^{M-K} N_K \frac{[(2J_1+1)(2J_2+1)]^{1/2}}{2} \times \begin{pmatrix} J_2 & J_1 & n \\ M & -M & 0 \end{pmatrix}\begin{pmatrix} J_2 & J_1 & n \\ K & -K & 0 \end{pmatrix} \quad (7)$$

where N_K and N_M are a nuclear statistical weight and degeneracy for each value of *M*, respectively. The rotational temperature is well established to be 0.37 K.[54]

The variational calculations were converged for the "4 + 1" pentamer by including states up to $J = 12$. We made use of the ab initio methods (MP2/6-311++G(3df,3pd)) to calculate the rotational constants, *A*, *B*, and *C*, and the permanent dipole moment, μ_p, for the "4 + 1" structure. The resulting rotational constants for the isolated molecule are 0.1358 cm^{-1}, 0.03736 cm^{-1}, and 0.02928 cm^{-1}, respectively. The permanent dipole moment does not point directly along the *A* axis of the complex, but instead has components (2.7376, 0.0960, 0.0253) Debye. The ab initio rotational constants must be modified to include the effects of the helium solvent before they can be used in the above analysis. For moderately heavy molecules of the type considered here, the rotational constants are observed to decrease by a factor of approximately three upon solvation in helium.[55] Although there is some scatter in these ratios, this turns out not to be a serious problem because the orientation distributions are only weakly dependent upon the values of the rotational constants at the fields used in the present experiments. Indeed, in the limit of infinite field, the dipole moment is precisely oriented with the field and the results become independent of the rotational constant and the the magnitude of the permanent dipole moment. As a result, we can proceed with the analysis of the data by simply assuming that the helium rotational constants are just the ab initio values, divided by a factor of 3. Similarly, the ab initio estimate of the magnitude of the permanent dipole moment is sufficient for this analysis. In contrast, any errors in the direction of the permanent dipole moment will translate into an error in the VTMAs. For this reason, we carried out a rather extensive study of how the permanent dipole moment direction changes with basis set. This revealed that the values converged rather quickly with increasing basis set size to the value used here.

Figure 4 shows the five H−F stretching modes of the "4 + 1" complex, along with the corresponding ab initio calculated VTMAs and the calculated permanent dipole moment direction. The local mode nature of the band at 3876.1 cm^{-1} is evident from the fact that the vibrational displacement vector

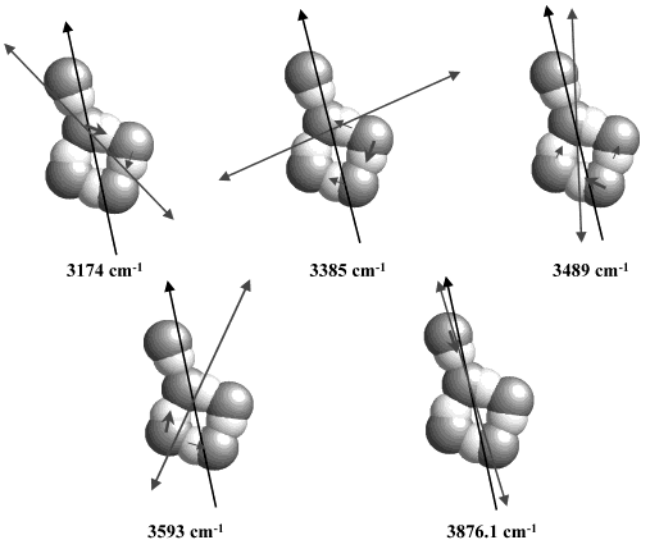

Figure 4. The calculated VTMAs (with respect to the permanent dipole moment) for the various HF stretching modes of the "4 + 1". The bands 3489 cm^{-1} and 3876.1 cm^{-1} have VTMAs with significant projections onto the permanent dipole moment, whereas the mode at 3385 cm^{-1} has a VTMA that is nearly perpendicular to the permanent dipole moment. The VTMAs for the vibrational modes at 3174 and 3593 cm^{-1} fall between these two extremes. The smaller arrows indicate the stretching motions associated with the normal mode vibrations.

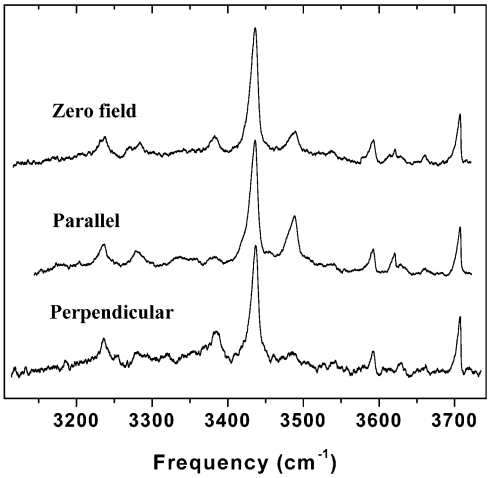

Figure 5. A comparison between the zero-field spectrum and spectra recorded in the presence of a large static electric field. The laser polarization was aligned either parallel or perpendicular to the applied field, as indicated.

is essentially parallel to the associated transition moment. In contrast, the ring modes involve the motion of multiple hydrogen atoms and the transition moment directions are not as easily visualized in terms of the displacement vectors. It is clear from this figure that VTMAs vary considerably, which helps considerably in assigning the spectrum.

The spectra used to determine the experimental VTMAs are shown in Figures 5 and 6, namely, those obtained with zero field and with the field on and the laser polarization directed either parallel or perpendicular to the DC field. Clearly, parallel fields enhance some of the bands, while others increase in intensity upon application of an electric field in the perpendicular configuration. The highest frequency mode (Figure 6) is assigned (from the scaled ab initio frequencies) to the H−F stretch of the molecule bound to the outside of the cyclic tetramer ring. According to the results in Figure 4, this band should be essentially parallel, consistent with the fact that we see a substantial increase in the signal levels upon the application of

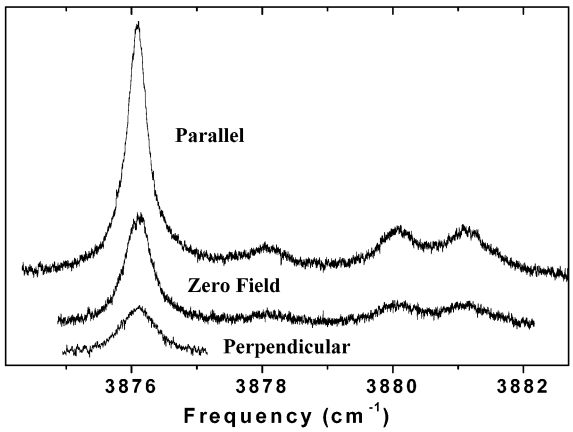

Figure 6. An expanded view of the highest-frequency vibrational mode of the "4 + 1" complex, corresponding to the HF stretch of the outside molecule. The laser polarization was aligned either parallel or perpendicular to the applied field, as indicated. The most intense peak in the spectrum is assigned to the "4 + 1" complex, while the weaker bands are attributed to clusters larger than $n = 5$.

the electric field in the parallel configuration. In contrast, the signal level of the band centered at 3385 cm^{-1} is diminished upon application of the parallel field, but enhanced by the application of a perpendicular field. The reverse is observed for the band centered at 3489 cm^{-1}. These bands are calculated to be primarily perpendicular and parallel, respectively, in excellent agreement with the experimental results. The lowest frequency band (3174 cm^{-1}) is only weakly observed in the experimental spectrum, but appears to be parallel, again in agreement with the calculated results. It is interesting to note that the band at 3593 cm^{-1} is rather unaffected by the electric field. At first sight this suggests that this band is associated with a nonpolar complex. However, the ab initio calculations reveal that this band of the "4 + 1" complex has a VTMA that is close to the "magic" angle, where the effects of the perpendicular and parallel components exactly cancel ($\alpha_{magic} = 54.75$ degrees). Close inspection reveals that there is a slight enhancement of the signal intensity upon application of the parallel field, as expected since the predicted VTMA is 39.7 degrees.

The experimental VTMAs can now be determined with the aid of the curve in Figure 7, which shows the polarization ratios as a function of the angle α. The dashed curve in the figure corresponds to a calculation using the ab initio rotational constants (i.e., not dividing by a factor of 3). From this it is clear that the errors associated with estimating the solvent effect on the rotational constants will have little effect on the VTMAs, particularly for the larger angles. The experimental polarization ratios for the four vibrational bands that have reasonable signals are shown as horizontal bars in the figure. The results of this analysis are summarized in Table 1. Overall, the agreement between experiment and theory is quite good, although somewhat worse than we observed previously for nucleic acid bases.[48] In part, this is because the vibrational bands in the present spectra are much broader and ride on top of a broad background that dramatically increases in intensity at higher HF pressures, the implication being that larger clusters have even broader absorption spectra throughout this region of the spectrum. This background makes the integration of the band intensities subject to increased errors, accounting for the fact that the average difference between the experimental and calculated angles is roughly a factor of 3 larger than in our previous study. What is surprising, however, is the fact that the highest-frequency band, where there are no background problems, has the poorest

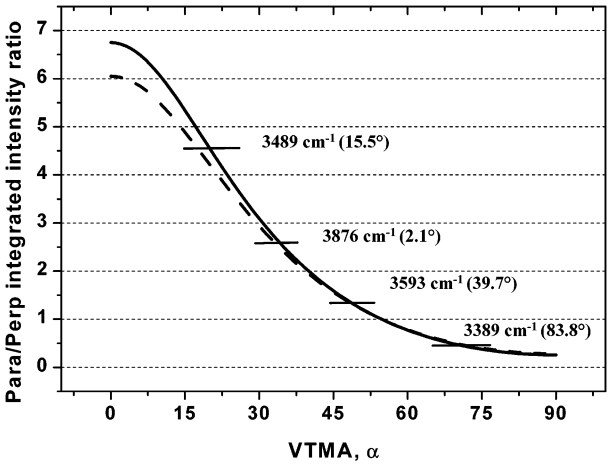

Figure 7. The parallel/perpendicular integrated intensity ratio, $\rho(\alpha)$, calculated from the dipole distribution function for the "4 + 1" isomer. The dashed curve was calculated using the ab initio rotational constants, without correcting for the effects of the helium. The solid curve corresponds to the calculation upon scaling the ab initio rotational constants by a factor of 3. The values for the vibrational transition moment angles obtained at the MP2/6-311++G(3df,3pd) level of theory are included in parentheses.

agreement, the difference being 33°. As discussed below, this disagreement is most likely indicative of other dynamical processes unique to this vibrational band.

Five additional bands are observed in the above spectra, at 3225, 3280, 3878.0, 3880.1, and 3881.2 cm^{-1}. All of these correspond to polar complexes, and the pick-up cell pressure dependence of the signals suggests that these bands are associated with complexes larger than $n = 5$. The band at 3878.0 cm^{-1} is so weak that an accurate determination of the associated cluster size was not possible. A number of "4 + 2" structures are indeed local minima on the $(HF)_6$ potential energy surface,[30,31] and ab initio calculations are underway in an effort to assign these bands.

Discussion

We begin this section by summarizing the important results presented in the previous section. First, we find that a fourth HF molecule can insert into a preformed cyclic trimer, resulting in the formation a cyclic tetramer. The implication is that the barrier to this process is quite low. We are assuming here, of course, that the helium relaxes the system during cluster formation, such that the system cannot cross barriers of any significant size. In fact, the observation of the cyclic tetramer alone would not enable us to confidently differentiate between (i) the case where the barrier is small and the system cold, and (ii) the case where the barrier is higher and the helium has not yet cooled the system. Fortunately, the pentamer results provide us with evidence that the cooling is effective and that we can stabilize the "4 + 1" complex. The implication here is that the barrier for the "4 + 1" system is larger than that for "3 + 1". This makes qualitative sense, given that the HF trimer is quite highly strained,[44,45] making it easier for the fourth HF to open the ring. The cyclic tetramer, on the other hand, has almost no ring strain[19] and will therefore be more difficult to open.

It is important to point out that although the "4 + 1" structure observed here is predicted to be the next-lowest energy isomer after the cyclic pentamer,[26,30] it has not been observed in a free-jet expansion.[21] Apparently the cooling in a free-jet expansion is too slow to stabilize this isomer, providing the system with enough time while it is warm to anneal to the globally stable ring structures.

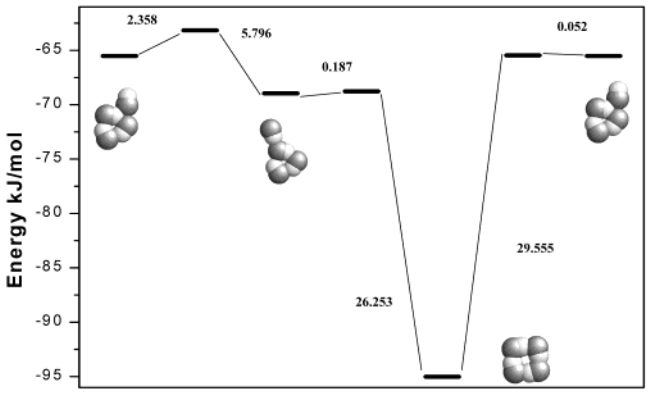

Figure 8. An energy diagram showing the transition states and minima on the $(HF)_4$ potential energy surface, as calculated in ref 26. Note that the highest barrier to rearrangement of the "3 + 1" complex to form the cyclic tetramer is 0.187 kJ/mol (16.6 cm^{-1}).

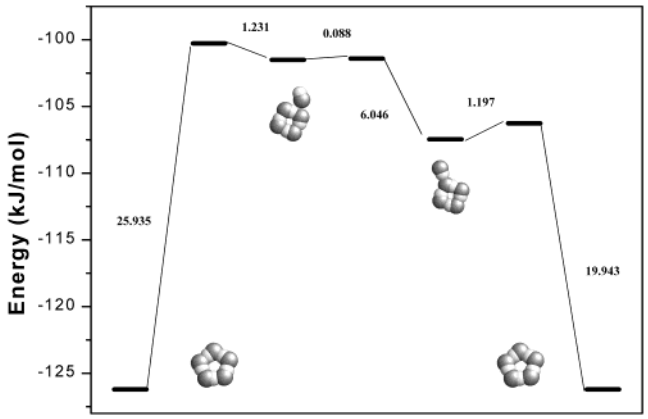

Figure 9. An energy diagram showing the transition states and minima on the $(HF)_5$ potential energy surface, as calculated in ref 26. Note that the barrier to rearrangement of the "4 + 1" complex to form the cyclic pentamer is 1.197 kJ/mol (100.1 cm^{-1}).

The present results can be examined in light of the recent theoretical calculations of Hodges et al.,[26] which provide not only the relative energies of the various isomers, but also the transition states between them. Figures 8 and 9 show energy diagrams summarizing the results of these calculations. It is immediately apparent that the barrier to ring insertion is larger for the "4 + 1" complex (100.1 cm^{-1}), compared to the "3 + 1" complex (16.6 cm^{-1}). It is interesting to note that the barrier for ring insertion from the higher energy "4 + 1" complex (where the outside molecule acts as an acceptor) is of similar magnitude. On the other hand, the barrier corresponding to rearrangement between the two "4 + 1" structures is so small (7.4 cm^{-1}) that it is unlikely we would ever see this higher-energy isomer.

The relative energies given in Figures 8 and 9 do not include the effects of zero-point energy. In a previous study of ring insertion in water complexes,[4] we found that the inclusion of zero-point energy tended to decrease the height of the barriers even further. It is thus conceivable that the "3 + 1" system is essentially barrierless. A similar analysis for these HF complexes is clearly needed. It is important to emphasize here that the energy of the "4 + 1" complex is approximately 1570 cm^{-1} higher than that of the cyclic pentamer. These results clearly demonstrate that the kinetics associated with helium droplet growth are such that even small barriers in the entrance channel are sufficient to result in the formation of highly metastable species that would not be formed in an environment that was anything like thermal.

We now return to the issue of the qualitative disagreement between the experimental and calculated VTMAs for the H−F stretch associated with the HF molecule on the outside of the ring in the "4 + 1" complex. There are a number of processes that could account for this large deviation. For example, since the ab initio VTMA calculation involves the harmonic approximation, errors may exist due to the neglect of the anharmonicity of this mode. Also, if a vibrational mode is strongly mixed with other vibrational states of the molecule, through anharmonic terms in the potential surface, which are clearly not included in the ab initio calculations, the experimental results would reflect this coupling. Indeed, a strongly mixed set of vibrations would display a VTMA intermediate between those of the pure states involved in the interaction. The fact that the "dangling" molecule is likely to undergo much larger amplitude motions than the molecules in the ring might indeed facilitate such coupling. It is interesting to note that calculated VTMAs for the bending degrees of freedom of the "4 + 1" complex are all large, corresponding to nearly perpendicular transitions. Thus, if the states to which the H−F stretch couple involve these low-frequency bending modes, a larger experimental VTMA, compared to the calculated value, would be expected.

The other possibility is that the outside HF molecule undergoes sufficiently wide amplitude bending motions that the calculated VTMA, determined from the equilibrium structure, is not appropriate for comparison with the experimental (vibrationally averaged) value. A rigorous theory for this vibrational averaging would require solving for the full, multidimensional dynamics of this system. Although such a calculation is beyond the scope of the present study, a qualitative assessment of the magnitude of this effect was explored by calculating the local bending potential of this "dangling" HF molecule, at the MP2 /6-311++G(3df,3pd) level of theory. VTMAs were also calculated at the various geometries. Overall the potential obtained from this is quite steep, suggesting that the amplitudes of the associated bending motions and the variation in the VTMAs with bending are considerably less than the difference between the experimental and calculated VTMAs for this mode.

Summary

We have made use of a new experimental method, based upon the measurement of VTMAs, to study the formation of HF clusters in helium nanodroplets. We find that insertion of an HF molecule into a preformed ring is essentially barrierless for the cyclic trimer, resulting in the formation of a cyclic tetramer. On the other hand, formation of the cyclic pentamer does not occur via ring insertion into the cyclic tetramer, but rather we observe the formation of a pentamer consisting of a tetramer ring with a "dangling" HF molecule, hydrogen-bonded to a fluorine atom in the ring. The assignment of the spectra for this complex is based upon comparing both the experimental vibrational frequencies and the associated VTMAs with the results of ab initio calculations. In three of the four bands, the agreement between theory and experiment is excellent, providing a convincing assignment. For the H−F stretch associated with the "dangling" HF molecule, the agreement is much poorer, which we tentatively explain in terms of anharmonic coupling of this vibration to combination states associated with the lower-frequency bending vibrations of the complex. This study provides semiquantitative information concerning how hydrogen-bond networks rearrange. The results are in good agreement with the potential surfaces reported previously.[26] The results suggest that barriers less than 100 cm^{-1} in height are sufficient to trap a system in a local minimum when helium is used as a heat bath. Further work is underway in identifying noncyclic complexes for $n > 5$, composed of a tetramer ring with multiple "dangling" HF molecules attached. The method of determining the experimental transition moment directions described here is shown to be useful in assigning complex vibrational spectra, and the potential for this technique to provide additional insight into the dynamics of intermode coupling is illustrated.

Acknowledgment. This work was supported by the National Science Foundation (CHE-99-87740). The North Carolina Supercomputing Center is also acknowledged for the computational resources needed for this work. We thank Wei Kong for providing the program for calculating the dipole distributions.

References and Notes

(1) Nauta, K.; Moore, D. T.; Miller, R. E. *Faraday Discuss.* **1999**, *113*, 261−278.
(2) Nauta, K.; Miller, R. E. *Science* **1999**, *283*, 1895−1897.
(3) Nauta, K.; Miller, R. E. *Science* **2000**, *287*, 293−295.
(4) Burnham, C. J.; Xantheas, S. S.; Miller, M. A.; Applegate, B. E.; Miller, R. E. *J. Chem. Phys.* **2002**, *117*, 1109−1122.
(5) Dyke, T. R.; Howard, B. J.; Klemperer, W. *J. Chem. Phys.* **1972**, *56*, 2442−2454.
(6) Lafferty, W. J.; Suenram, R. D.; Lovas, F. J. *J. Mol. Spectrosc.* **1987**, *123*, 434−452.
(7) Pine, A. S.; Lafferty, W. J. *J. Chem. Phys.* **1983**, *78*, 2154−2162.
(8) Huang, Z. S.; Jucks, K. W.; Miller, R. E. *J. Chem. Phys.* **1986**, *85*, 3338−3341.
(9) Anderson, D. T.; Davis, S.; Nesbitt, D. J. *J. Chem. Phys.* **1996**, *105*, 4488−4503.
(10) Anderson, D. T.; Davis, S.; Nesbitt, D. J. *J. Chem. Phys.* **1996**, *104*, 6225−6243.
(11) Puttkamer, K. v.; Quack, M.; Suhm, M. A. *Mol. Phys.* **1988**, *65*, 1025−1045.
(12) Bohac, E. J.; Marshall, M. D.; Miller, R. E. *J. Chem. Phys.* **1992**, *96*, 6681−6695.
(13) Marshall, M. D.; Bohac, E. J.; Miller, R. E. *J. Chem. Phys.* **1992**, *97*, 3307−3317.
(14) Klopper, W.; Quack, M.; Suhm, M. A. *J. Chem. Phys.* **1998**, *108*, 10096−10115.
(15) Nauta, K.; Miller, R. E. *J. Chem. Phys.* **2000**, *113*, 10158−10168.
(16) Michael, D. W.; Lisy, J. M. *J. Chem. Phys.* **1986**, *85*, 2528−2537.
(17) Suhm, M. A.; Farrell, J. T., Jr.; Ashworth, S. H.; Nesbitt, D. J. *J. Chem. Phys.* **1993**, *98*, 5985−5989.
(18) Suhm, M. A.; Nesbitt, D. J. *Chem. Soc. Rev.* **1995**, *24*, 45−54.
(19) Quack, M.; Schmitt, U.; Suhm, M. A. *Chem. Phys. Lett.* **1993**, *208*, 446−452.
(20) Luckhaus, D.; Quack, M.; Schmitt, U.; Suhm, M. A. *Ber. Bunsen.-Ges.* **1995**, *99*, 457−468.
(21) Oudejans, L.; Miller, R. E. *J. Chem. Phys.* **2000**, *113*, 971−978.
(22) Quack M.; Suhm, M. A. *Advances in Molecular Vibrations and Collision Dynamics, Vol. 3*; JAI Press: Greenwich, 1998; pp 205−248.
(23) Huisken, F.; Kaloudis, M.; Kulcke, A.; Laush, C.; Lisy, J. M. *J. Chem. Phys.* **1995**, *103*, 5366−5377.
(24) Quack, M.; Schmitt, U.; Suhm, M. A. *Chem. Phys. Lett.* **1997**, *269*, 29−38.
(25) Karpfen, A. *Int. J. Quantum Chem.* **1990**, *24*, 129−140.
(26) Hodges, M. P.; Stone, A. J.; Lago, E. C. *J. Phys. Chem. A* **1998**, *102*, 2455−2465.
(27) Zhang, C.; Freeman, D. L.; Doll, J. D. *J. Chem. Phys.* **1989**, *91*, 2489−2497.
(28) Maerker, C.; Schleyer, P. V. R.; Liedl, K. R.; Ha, T.-K.; Quack, M.; Suhm, M. A. *J. Comput. Chem.* **1997**, *18*, 1695−1719.
(29) Ovchinnikov, M.; Apkarian, V. A. *J. Chem. Phys.* **1999**, *110*, 9842−9852.
(30) Grigorenko, B. L.; Moskovsky, A. A.; Nemukhin, A. V. *J. Mol. Struct. (THEOCHEM)* **2000**, *498*, 47−60.
(31) Grigorenko, B. L.; Moskovsky, A. A.; Nemukhin, A. V. *J. Chem. Phys.* **1999**, *111*, 4442−4452.
(32) Blake, T. A.; Sharpe, S. W.; Xantheas, S. S. *J. Chem. Phys.* **2000**, *113*, 707−718.
(33) Frisch, M. J.; Trucks, G. W.; Schlegel, H. B.; Scuseria, G. E.; Robb, M. A.; Cheeseman, J. R.; Zakrzewski, V. G.; Montgomery, J. A., Jr.; Stratmann, R. E.; Burant, J. C.; Dapprich, S.; Millam, J. M.; Daniels, A. D.; Kudin, K. N.; Strain, M. C.; Farkas, O.; Tomasi, J.; Barone, V.; Cossi, M.; Cammi, R.; Mennucci, B.; Pomelli, C.; Adamo, C.; Clifford, S.; Ochterski, J.; Petersson, G. A.; Ayala, P. Y.; Cui, Q.; Morokuma, K.; Malick,

D. K.; Rabuck, A. D.; Raghavachari, K.; Foresman, J. B.; Cioslowski, J.; Ortiz, J. V.; Stefanov, B. B.; Liu, G.; Liashenko, A.; Piskorz, P.; Komaromi, I.; Gomperts, R.; Martin, R. L.; Fox, D. J.; Keith, T.; Al-Laham, M. A.; Peng, C. Y.; Nanayakkara, A.; Gonzalez, C.; Challacombe, M.; Gill, P. M. W.; Johnson, B. G.; Chen, W.; Wong, M. W.; Andres, J. L.; Head-Gordon, M.; Replogle, E. S.; Pople, J. A. *Gaussian 98*; Gaussian, Inc.: Pittsburgh, PA, 1998.

(34) Nauta, K.; Miller, R. E. *J. Chem. Phys.* **1999**, *111*, 3426−3433.

(35) Knuth, E. L.; Schilling, B.; Toennies, J. P. "On Scaling Parameters for Predicting Cluster Sizes in Free Jets. 19th International Symposium on Rarefied Gas Dynamics, 1995.

(36) Lewerenz, M.; Schilling, B.; Toennies, J. P. *Chem. Phys. Lett.* **1993**, *206*, 381−387.

(37) Hartmann, M.; Miller, R. E.; Toennies, J. P.; Vilesov, A. F. *Science* **1996**, *272*, 1631−1634.

(38) Brink, D. M.; Stringari, S. *Z. Phys. D* **1990**, *15*, 257−263.

(39) Block, P. A.; Bohac, E. J.; Miller, R. E. *Phys. Rev. Lett.* **1992**, *68*, 1303−1306.

(40) Rost, J. M.; Griffin, J. C.; Friedrich, B.; Herschbach, D. R. *Phys. Rev. Lett.* **1992**, *68*, 1299−1301.

(41) Kolenbrander, K. D.; Dykstra, C. E.; Lisy, J. M. *J. Chem. Phys.* **1988**, *88*, 5995−6012.

(42) Dykstra, C. E. *J. Phys. Chem.* **1990**, *94*, 180−185.

(43) Sun, H.; Watts, R. O.; Buck, U. *J. Chem. Phys.* **1992**, *96*, 1810−1821.

(44) Suhm, M. A. *Ber. Bunsen-Ges.* **1995**, *99*, 1159−1167.

(45) Klopper, W.; Quack, M.; Suhm, M. A. *Mol. Phys.* **1998**, *94*, 105−119.

(46) Quack, M.; Stohner, J.; Suhm, M. A. *J. Mol. Struct.* **1993**, *294*, 33−36.

(47) Quack, M.; Stohner, J.; Suhm, M. A. *J. Mol. Struct.* **2001**, *599*, 381−425.

(48) Dong, F.; Miller, R. E. *Science* **2002**, *298*, 1227−1230.

(49) Franks, K. J.; Li, H. Z.; Kong, W. *J. Chem. Phys.* **1999**, *110*, 11779−11788.

(50) Castle, K. J.; Abbott, J.; Peng, X.; Kong, W. *J. Chem. Phys.* **2000**, *113*, 1415−1419.

(51) Castle, K. J.; Kong, W. *J. Chem. Phys.* **2000**, *112*, 10156−10161.

(52) Kong, W.; Bulthuis, J. *J. Phys. Chem. A* **2000**, *104*, 1055−1063.

(53) Hongzhi, L.; Franks, K. J.; Hanson, R. J.; Kong, W. *J. Phys. Chem. A* **1998**, *102*, 8084−8090.

(54) Hartmann, M.; Miller, R. E.; Toennies, J. P.; Vilesov, A. F. *Phys. Rev. Lett.* **1995**, *75*, 1566−1569.

(55) Callegari, C.; Lehmann, K. K.; Schmied, R.; Scoles, G. *J. Chem. Phys.* **2001**, *115*, 10090−10110.